SCIENCE CHINA
Physics, Mechanics & Astronomy

•Article•

July 2020 Vol. 63 No. 7: 276113
https://doi.org/10.1007/s11433-020-1535-3

Abnormal relaxation kinetics in D-mannitol glass confined by nanoporous alumina

YaRu Cao[1,2,3], LiJian Song[2,3], Ao Li[2,3], JunTao Huo[2,3], FuShan Li[4], Wei Xu[2,3*], and Jun-Qiang Wang[2,3*]

[1] *College of Materials Science and Chemical Engineering, Ningbo University, Ningbo 315211, China;*
[2] *CAS Key Laboratory of Magnetic Materials and Devices, Zhejiang Province Key Laboratory of Magnetic Materials and Application Technology, Ningbo Institute of Materials Technology and Engineering, Chinese Academy of Sciences, Ningbo 315201, China;*
[3] *Center of Materials Science and Optoelectronics Engineering, University of Chinese Academy of Science, Beijing 100049, China;*
[4] *School of Materials Science and Engineering, Zhengzhou University, Zhengzhou 450001, China*

Received January 1, 2020; accepted February 24, 2020; published online March 30, 2020

The relaxation kinetics and phase transformations of the confined D-mannitol (DM) in nanoporous alumina are studied *in-situ* using a high-precision nano-calorimeter. We find that the crystallization behavior can be suppressed when it is confined in nanopores smaller than 50 nm. The confined DM glass has a much smaller fragility (~76) than free DM glass (~125), confirming the enhanced glass-forming ability. It is intriguing that during isothermal annealing both the confined and free DM glasses relaxation kinetics experience two relaxation stages that have distinct activation energies. The relaxation activation energy of the confined glass is about 25%-29% smaller than the free glass, which is attributed to the reduced dimensionality. The abnormal kinetics observed in the confined DM glass open a new avenue for preparing stable glasses.

D-mannitol glass, confinement, relaxation, crystallization

PACS number(s): 61.43.Fs, 61.20.Lc, 64.70.Pf

Citation: Y. R. Cao, L. J. Song, A. Li, J. T. Huo, F. S. Li, W. Xu, and J.-Q. Wang, Abnormal relaxation kinetics in D-mannitol glass confined by nanoporous alumina, Sci. China-Phys. Mech. Astron. **63**, 276113 (2020), https://doi.org/10.1007/s11433-020-1535-3

1 Introduction

Owing to the nonequilibrium nature, glasses usually exhibit plenty of relaxations, and phase transformations [1,2]. In recent decades, the size-dependent kinetics of various glassy materials have attracted extensive research interests. For example, the surface atoms diffuse much faster compared to the inner bulk atoms [3-5]. The enhanced surface diffusion is attributed to the vanishing of intermolecular coupling in the surface [5]. Glasses confined in nanometer-scale can exhibit abnormal crystallization and relaxation kinetics that are not observed in bulk systems [6-11]. For example, the nucleation kinetics of glassy isotactic polypropylene transform from heterogeneous to homogeneous along with the decrease of nanoconfinement size [9]. If the nanopore size is smaller than the critical nucleus size, the crystallization may be suppressed [9,10]. On the other hand, the molecular relaxation kinetics can be modulated in two opposite ways that affect the growth of crystals [12]. The bulk-like relaxation kinetics become faster [13] to accelerate crystal growth [14], whereas the interfacial relaxation kinetics may become slower to reduce crystal growth [10]. Thus, it is still open and challenging to design glasses with desirable thermal stability

*Corresponding authors (Jun-Qiang Wang, email: jqwang@nimte.ac.cn; Wei Wu, email: weixu@nimte.ac.cn)

using nano-confinement.

D-mannitol (DM) is a glass-forming hydrgen-bonded polyalcohol. Owing to its non-hygroscopicity, quick-drying and good chemical stability characteristics, it has been widely applied in pharmaceuticals, such as anticancer drugs, antibacterial drugs, antihistamines, and hyperosmotic antihypertensive drugs [15]. Glassy state is superior in pharmaceutical applications because it dissolves faster and has higher solubility compared to crystalline counterparts [16]. Interestingly, the DM exhibits polyamorphism upon annealing [17,18]. The new glassy phase X exhibits 30 K higher glass transition temperature (T_g) and lower density compared to the as-cooled glass [17]. The polyamorphism transformation is attributed to the competition between hydrogen bonding and van der Waals attraction [17]. Although phase X has a higher T_g, its crystallization tendency was not suppressed and its application as glassy pharmaceuticals was hampered. Thus, it is still an intriguing question how the nanoconfinement influences the relaxation and crystallization kinetics of glassy DM.

2 Experimental section

DM (purity > 99 wt.%) was purchased from Sigma Company. The nanoporous AAO membranes with different nanopore sizes were purchased from Shangmu Company. The DM was fused at 156°C and adsorbed into the AAO membranes to obtain the confined sample. The surface of the filled membrane was cleaned with ethanol to remove the leftover DM on the surface. Isothermal annealing experiments were performed *in situ* using a high-precision and high-rate differential scanning nano-calorimeter (F-DSC, Flash DSC 1, Mettler Toledo) [19,20]. A small piece of sample was cut from the membranes under an optical microscope and then transferred onto the F-DSC chip. During measurement, a flow of high-purity Ar gas (40 mL/min) was applied to protect the sample from oxidation. The morphology was examined using a scanning electronic microscope (SEM, Thermo scientific, Verios G4 UC). The atomic packing structure was studied using X-ray diffraction (XRD) in a reflection mode (Bruker D8 Advance Davinci). The molecular vibration spectrum was investigated using micro-FTIR (Agilent, Cary660+620).

3 Results and discussion

The SEM images (Figure 1(a)-(d)) show that the diameters of the nanopores in AAO templates are about 30 nm (D30), 50 nm (D50), 90 nm (D90), and 200 nm (D200), respectively. Figure 1(e)-(h) show images of AAOs filled with DM. It confirms that DM has been filled homogeneously in nanopores.

Figure 2(a) shows the cooling DSC traces at a rate of 5 K/s for the free DM and confined DM. The free DM exhibits a large exothermic crystallization peak with an onset crystallization temperature T_x at about 367 K. For the confined

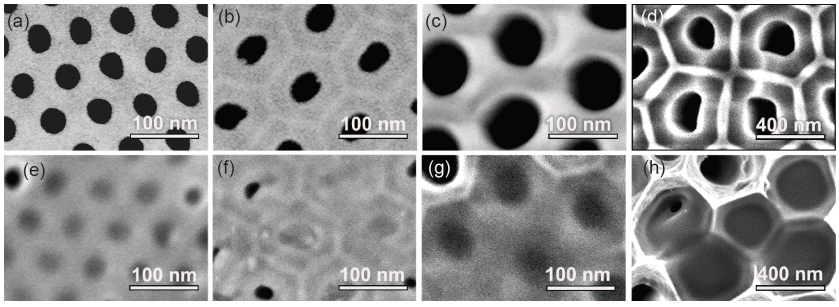

Figure 1 SEM images of (a)-(d) empty nanoporous AAO templates, and AAO templates with confined D-mannitols ((e) D30, (f) D50, (g) D90, (h) D200).

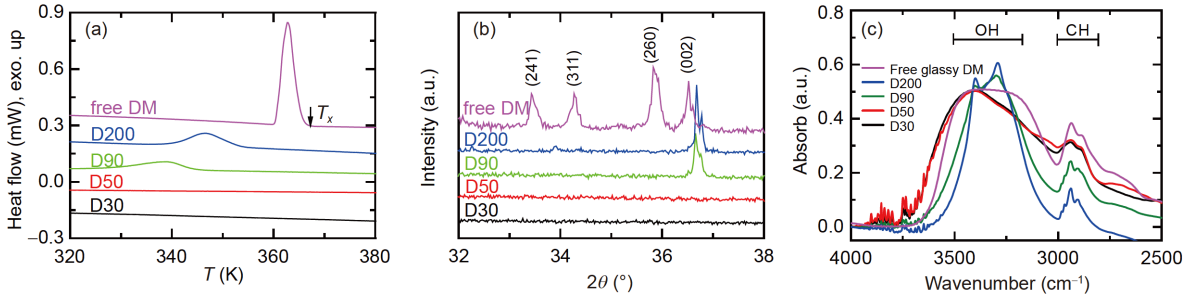

Figure 2 (Color online) (a) Cooling DSC traces at 5 K/s; (b) XRD curves for free DM and DM confined in nanoporous AAO with pore diameters ranging from 200 to 30 nm; (c) infrared spectra of free glassy D-mannitol and confined D-mannitols.

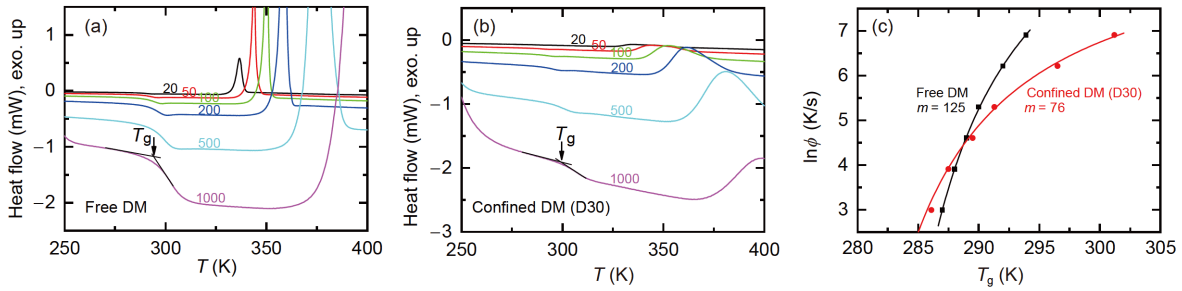

Figure 3 (Color online) The heating DSC traces of (a) free DM and (b) D30 confined DM at various heating rates. The onset temperatures for glass transition (T_g) is indicated by the crossing of two tangent lines and marked by arrows. (c) The heating rate as a function of glass transition temperature. The solid curves are fitting results using VFT equation, which yields a fragility of about 125 for free DM and 76 for D30 confined DM, respectively.

nanoporous AAO, the crystallization peak has been postponed to lower temperatures, with T_x = 353 K for D200 and T_x = 344 K for D90, respectively. For the D50 and D30 confined samples, the crystallization has been suppressed completely, indicating the formation of glass.

Figure 2(b) shows XRD curves of the confined DM. All samples were melted at 156°C for 3 min and then cooled to 25°C at a rate about 5 K/s. For the D90 and D200 confined DM, there are obvious crystalline diffraction peaks. But for the D50 and D30 confined DM, there is no sharp diffraction peak that suggests a glassy state. It suggests that the nanoporous confinement has strong effect in suppressing the crystallization. When the pore size is as small as 50 nm, the crystallization has been suppressed completely with greatly enhanced glass-forming ability.

To reveal the influence of confinement on the molecular interactions, FTIR experiments were performed, as shown in Figure 2(c). The OH stretch and CH stretch vibration modes in the fundamental frequency region (2500-4000 cm^{-1}) change a lot for the confined samples. The D200 sample exhibits sharp crystalline vibration peaks. With the decrease of the nanopore size, OH peak becomes broader and gradually shifts to higher wavenumbers. For the D50 and D30 sample, the fine structures in the OH stretching mode disappear and exhibit amorphous peak morphology. Compared to the free DM glass, the D50 and D30 confined glasses exhibit more high-frequency and less low-frequency vibrations for the OH stretching mode, which is attributed to the frustration of hydrogen bonds in the confined samples.

Figure 3(a) and (b) show the DSC traces for the free and confined DM glasses upon heating. For the confined DM, the crystallization onset temperature does not change very much compared to the free DM, which suggests that the crystal nucleation is not influenced. This is different from former works [9,10] that nanoconfinement would influence the crystal nucleation kinetics. The exothermic peak is wider than the free DM glass, which suggests slower crystal growth in the confined DM glass. Figure 3(c) shows the glass transition onset temperature (T_g) at various heating rates. It is interesting that T_g is close to each other for the free DM and confined DM at low heating rates, while the T_g of confined DM increases fast at high heating rates. To evaluate the kinetic characteristic of glass transition, the fragility (m) of the glass-forming liquid is studied according to the Vogel-Fulcher-Tammann (VFT) equation [21], $\ln\varphi = \ln A + DT_0/(T - T_0)$, with fragility $m = DT_0T_g/(T_g - T_0)^2\ln 10$. The fragility of confined DM is determined to be about 76, which is a much stronger liquid characteristic than the free DM with m = 125. The large decrease in fragility for the confined DM suggests an increase in the glass-forming ability [22], which is consistent with the data in Figure 2.

The relaxation kinetics upon isothermal annealing was studied, as shown in Figure 4. Figure 4(a) shows the DSC traces for the as-cooled confined glass and the confined glass that was pre-annealed at 273 K for 1000 s. After the relaxation at 273 K for 1000 s, an excess endothermic peak appears close to T_g. The endothermic peak is obtained by subtracting the heat flow of the as-cooled sample, as shown in Figure 4(a). To further reveal the relaxation kinetics, the heating rate-dependent behavior of the relaxation peak was studied, as shown in Figure 4(b). The relaxation peak shifts to higher temperatures with the increase of heating rate. The activation energy (ΔE) of the corresponding relaxation state was obtained by the slope in Kissinger plot, as shown in Figure 4(c).

It is interesting that both the free and confined DM glasses exhibit a two-step relaxation behavior. At the initial annealing stage, the ΔE is as small as about 70 kJ/mol for the free DM, which is attributed to the β relaxation mode ($\Delta E_\beta = 26RT_g \approx 60$ kJ/mol [23]). When the annealing time is long enough, ΔE increases to a much larger value, about 115 kJ/mol for the free DM. This is almost equal to the α relaxation activation energy 118 kJ/mol that is determined in the inset of Figure 4(d). Such a β-to-α two-step relaxation phenomenon has also been observed in metallic glasses [24].

The confined DM glass also exhibits a two-step relaxation, but has much smaller relaxation activation energy compared to the free DM. In confinement, the β relaxation activation energy is about 50 kJ/mol that is 29% smaller than the free

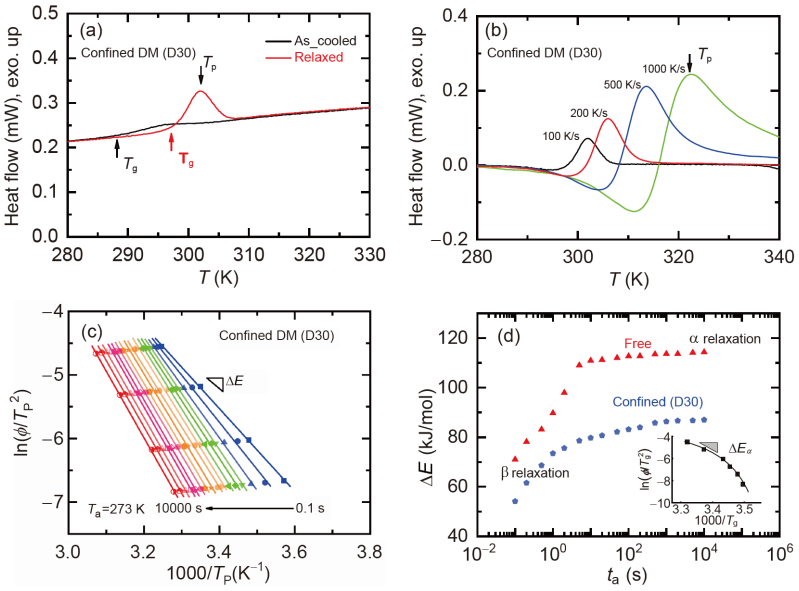

Figure 4 (Color online) (a) The DSC traces for the D30 confined sample. The relaxed sample is pre-annealed at 273 K for 1000 s. The heating rate is 100 K/s. T_p is relaxation peak temperature. (b) The heat flow traces of relaxation peak (T_a = 273 K, t_a = 1000 s) under different heating rates. (c) Kissinger relationship of the relaxation peak temperature when being annealed at T_a = 273 K for different annealing times (t_a = 0.1-10000 s). (d) The evolution of relaxation activation energy ΔE along with annealing time when being annealed at 273 K. Inset is the non-Arrhenius behavior of T_g fitted by VFT equation, from which the activation energy of relaxation can be determined.

DM, while the α relaxation activation energy is about 87 kJ/mol that is 25% smaller than the free DM. The decrease in relaxation activation energy is attributed to the reduced dimensionality for the confined sample.

Table 1 shows the characteristic thermal parameters of the two glassy states. Nano-confined DM exhibits higher T_g value which becomes pronounced at higher heating rates. The relaxation activation energy for confined DM is smaller than free DM. A similar result was also found in confined water [11]. This effect is primarily attributed to the size effect on the frustration of hydrogen bonds in the confined samples [11]. However, when the confined system has a strong interface effect, two layers are formed [25]. In such a case, the layer near the pore walls shows increased T_g due to the strong interfacial interaction, while the local packing density in the core volume would be reduced, which induces a decreased T_g. Based on the FTIR experiments, we propose that both the higher T_g and stronger liquid dynamics in AAO confined DMs are attributed to the frustration of hydrogen bonds. The decrease in relaxation activation energy could also be attributed to the reduced dimensionality for the confined sample.

Table 1 The characteristic thermal parameters of the free DM and confined DM. T_g is the value measured at heating rate of 1000 K/s

Composition	T_g (K)	m	ΔE_β (kJ/mol)	ΔE_α (kJ/mol)
Free DM	294.3	125	70	115
Confined DM (D30)	302.5	76	50	87

4 Conclusions

In this work, the crystallization behavior and relaxation kinetics of nano-confined D-mannitol glasses are studied. The crystallization for the D-mannitol confined in nanopores as small as 50 nm can be suppressed completely during cooling. The confined DM exhibits higher T_g value which becomes more pronounced at a higher heating rate. The confined glass-forming liquid is much stronger than the free material. A two-step β-to-α relaxations transformation phenomenon occurs during isothermal annealing for both confined and free systems, but the confined glass exhibits much smaller relaxation activation energy. These thermodynamic and kinetic properties in confined DMs could be explained by the frustration of hydrogen bonds dominated by size effect. These results verified that nano-confinement may be an applicable general strategy for enhancing the thermal stability of molecular glasses.

This work was supported by the National Key R&D Program of China (Grant Nos. 2018YFA0703602, and 2018YFA0703604), the National Natural Science Foundation of China (Grant Nos. 51701230, 51922102, and 51771216), Zhejiang Provincial Natural Science Foundation of China (Grant No. LR18E010002), and Ningbo Science and Technology Innovation 2025 Project (Grant No. 2019B10051).

1 L. J. Song, M. Gao, W. Xu, J. T. Huo, J. Q. Wang, R. W. Li, W. H. Wang, and J. H. Perepezko, Acta Mater. **185**, 38 (2020).
2 Z. Fakhraai, and J. A. Forrest, Science **319**, 600 (2008).
3 L. Zhu, C. W. Brian, S. F. Swallen, P. T. Straus, M. D. Ediger, and L.

Yu, Phys. Rev. Lett. **106**, 256103 (2011).
4 S. S. Jiang, K. F. Gan, Y. J. Huang, P. Xue, Z. L. Ning, J. F. Sun, and A. H. W. Ngan, Int. J. Plast. **125**, 52 (2020).
5 K. L. Ngai, S. Capaccioli, C. R. Cao, H. Y. Bai, and W. H. Wang, J. Non-Crystalline Solids **463**, 85 (2017).
6 L. D. Gelb, K. E. Gubbins, R. Radhakrishnan, and M. Sliwinska-Bartkowiak, Rep. Prog. Phys. **62**, 1573 (1999).
7 Q. Tang, W. Hu, and S. Napolitano, Phys. Rev. Lett. **112**, 148306 (2014).
8 S. Sohn, Y. Xie, Y. Jung, J. Schroers, and J. J. Cha, Nat. Commun. **8**, 1980 (2017).
9 H. Duran, M. Steinhart, H. J. Butt, and G. Floudas, Nano Lett. **11**, 1671 (2011).
10 X. Dai, H. Li, Z. Ren, T. P. Russell, S. Yan, and X. Sun, Macromolecules **51**, 5732 (2018).
11 J. Swenson, and J. Teixeira, J. Chem. Phys. **132**, 014508 (2010).
12 D. Richter, and M. Kruteva, Soft Matter **15**, 7316 (2019).
13 K. Chat, W. Tu, L. Laskowski, and K. Adrjanowicz, J. Phys. Chem. C **123**, 13365 (2019).
14 S. Ruan, W. Zhang, Y. Sun, M. D. Ediger, and L. Yu, J. Chem. Phys. **145**, 064503 (2016).
15 B. C. Saha, and F. M. Racine, Appl. Microbiol. Biotechnol. **89**, 879 (2011).
16 L. Yu, Adv. Drug Deliver. Rev. **48**, 27 (2001).
17 M. Zhu, J. Q. Wang, J. H. Perepezko, and L. Yu, J. Chem. Phys. **142**, 244504 (2015).
18 W. Tang, and J. H. Perepezko, J. Chem. Phys. **149**, 074505 (2018).
19 J. Q. Wang, Y. Shen, J. H. Perepezko, and M. D. Ediger, Acta Mater. **104**, 25 (2016).
20 J. Q. Wang, N. Chen, P. Liu, Z. Wang, D. V. Louzguine-Luzgin, M. W. Chen, and J. H. Perepezko, Acta Mater. **79**, 30 (2014).
21 R. Brüning, and K. Samwer, Phys. Rev. B **46**, 11318 (1992).
22 H. Tanaka, J. Non-Crystalline Solids **351**, 678 (2005).
23 L. Hu, and Y. Yue, J. Phys. Chem. C **113**, 15001 (2009).
24 L. Song, W. Xu, J. Huo, J. Q. Wang, X. Wang, and R. Li, Intermetallics **93**, 101 (2018).
25 L. Li, D. Zhou, D. Huang, and G. Xue, Macromolecules **47**, 297 (2014).